SUBSPACE-BASED CO-ARRAY PROCESSING FOR NESTED ARRAYS WITHOUT EIGENDECOMPOSITION

Xinghao Qu[1,2,3]*, Zhigang Shang*[1,2,3]*, Gang Qiao*[1,2,3]*, Jixing Qin*[4]*, and Xuerui Liu*[1,2,3]

[1]National Key Laboratory of Underwater Acoustic Technology, Harbin Engineering University, Harbin 150001, China
[2]Key Laboratory of Marine Information Acquisition and Security (Harbin Engineering University), Ministry of Industry and Information Technology, Harbin 150001, China
[3]College of Underwater Acoustic Engineering, Harbin Engineering University, Harbin 150001, China
[4]State Key Laboratory of Acoustics, Institute of Acoustics, Chinese Academy of Sciences, Beijing 100190, China

ABSTRACT

For the purpose of computational efficiency, we propose two subspace-based methods, but without eigendecomposition, to address the two typical problems in nested array processing, i.e., direction-of-arrival (DOA) estimation and noise elimination. In detail, to estimate DOA parameters, we judiciously arrange the segments extracted from the co-array model and then introduce a novel co-array-based orthogonal propagator method (COPM). Next, we develop a projection-based noise cancellation approach in the co-array domain, improving the relatively poor performance of COPM at low signal-to-noise ratios. Simulations evaluate the proposed algorithms under both overdetermined and underdetermined conditions.

***Index Terms*—** Co-array model, direction-of-arrival estimation, nested array, orthogonal propagator method.

1. INTRODUCTION

The nested array (NA) [1] and its variants have attracted much research interest over the years because such array geometries provide increased degrees of freedom. This appealing advantage is achieved in the co-array domain. Specifically, by vectorizing the covariance matrix, we can formulate the self-Khatri-Rao product of the array manifold matrix. This will yield a difference co-array (DCA) model that behaves like a measurement sample of an extended virtual uniform linear array (ULA). Then, many approaches can accommodate this DCA model to realize underdetermined (more sources than sensors) direction-of-arrival (DOA) estimation.

Among them, using the spatial smoothing (SS) technique to enable subspace-based DOA estimation algorithms (e.g., MUSIC) gains a trade-off between computational complexity and estimation precision, thus widely used [2–6]. In addition, it has been shown that the original SS step can be further simplified by the construction in [7], which is much easier to compute from array data and becomes an attractive option [8–13]. However, its basic idea is still to reconstruct a square covariance matrix. In fact, such an inflexible operation does not fully exploit the source number typically assumed as a priori knowledge in most subspace methods. In practice, the number of incident sources may not reach the identifiability bound of an NA. At this point, the aforementioned methods will suffer from an unnecessary loss of array aperture.

On the other hand, to obtain mutually orthogonal signal and noise subspaces, the conventional wisdom is to use eigenvalue decomposition (EVD). Unfortunately, EVD procedures handling high-dimensional matrices are computationally intensive and time-consuming, thereby unfavorable for the online processing of massive arrays. To overcome this problem, researchers have proposed subspace-based methods without eigendecomposition (SMWE) (e.g., the orthogonal propagator method (OPM) [14]), which have aroused much attention in recent decades [15–18]. However, these works only account for physical arrays rather than virtual co-arrays. It is worth mentioning that when it comes to the NA geometry, in which just a few physical sensors can generate a large virtual DCA, SMWE-type schemes will be more attractive.

Motivated by the above considerations, we propose a novel co-array-based OPM (COPM) tailored for NAs to estimate arrival angles. It uses the propagator matrix, which can be easily extracted from array data, to construct the signal or noise subspace, thus avoiding the EVD required by conventional subspace methods. Considering the sensitivity of COPM to additive noise, we also develop a projection-based noise elimination method (PNEM) without EVD. Finally, the numerical results verify the better performance of COPM over the conventional SS-based MUSIC (SS-MUSIC).

Notations: Matrices and vectors are represented as boldface capital and lowercase letters, respectively. $(\cdot)^T$, $(\cdot)^H$, $(\cdot)^*$, $(\cdot)^{-1}$, and $(\cdot)^\dagger$ denote transposition, conjugate transposition, complex conjugation, inverse, and pseudo-inverse, respectively. $\mathbf{0}_{M,N}$ and $\mathbf{I}_N$ stand for an $M \times N$ zero matrix and

This work was supported by the State Key Laboratory of Acoustics, Chinese Academy of Sciences under Grant SKLA202202. *(Corresponding author: Zhigang Shang.)*

an N-dimensional identity matrix, respectively. The Khatri-Rao product is denoted by $\odot$. $\mathbb{E}\{\cdot\}$, $\mathrm{vec}\{\cdot\}$, and $\mathrm{trace}\{\cdot\}$ are the statistical expectation, matrix vectorization, and matrix trace operators, respectively. $\mathrm{diag}\{\mathbf{X}\}$ returns a column vector composed of the diagonal elements in $\mathbf{X}$, and $\mathrm{diag}\{\mathbf{x}\}$ forms a diagonal matrix with the diagonal entries being $\mathbf{x}$.

2. DIFFERENCE CO-ARRAY MODEL

We consider that K (known as a priori or detected successfully) uncorrelated far-field narrowband sources, i.e., $\mathbf{s}(t) = [s_1(t), \ldots, s_K(t)]^T$, from directions $\boldsymbol{\theta} = \{\theta_1, \ldots, \theta_K\}$ impinge on an NA with N physical sensors located at positions $\mathcal{P}_N = \{d_1 = 0, d_2 = 1, \ldots, d_N\}$ (measured in half-wavelength units). The received data vector is given as

$$\mathbf{y}(t) = \mathbf{A}(\boldsymbol{\theta})\mathbf{s}(t) + \mathbf{n}(t), \tag{1}$$

where the N elements of the noise vector $\mathbf{n}(t)$ are assumed to be independent and identically distributed random variables. The manifold matrix $\mathbf{A}(\boldsymbol{\theta}) = \left[\mathbf{a}(\theta_1), \ldots, \mathbf{a}(\theta_K)\right]$ comprises K steering vectors $\mathbf{a}(\theta_k) = \left[1, e^{j\pi \sin\theta_k}, \ldots, e^{j\pi d_N \sin\theta_k}\right]^T$ $(k = 1, 2, \ldots, K)$. Then, assume that $\mathbf{s}(t)$ and $\mathbf{n}(t)$ are statistically independent. The covariance matrix of $\mathbf{y}(t)$ reads

$$\mathbf{R} = \mathbb{E}\left\{\mathbf{y}(t)\mathbf{y}^H(t)\right\} = \mathbf{A}(\boldsymbol{\theta})\mathbf{R}_s\mathbf{A}^H(\boldsymbol{\theta}) + \sigma_n^2\mathbf{I}_N, \tag{2}$$

where σ_n^2 is the variance of noise, and the diagonal matrix $\mathbf{R}_s = \mathrm{diag}\left\{\sigma_{s,1}^2, \sigma_{s,2}^2, \ldots, \sigma_{s,K}^2\right\}$ contains the powers of the K incident signals. Vectorizing $\mathbf{R}$, we have

$$\mathbf{r} = \mathrm{vec}\left\{\mathbf{R}\right\} = \left(\mathbf{A}^*(\boldsymbol{\theta}) \odot \mathbf{A}(\boldsymbol{\theta})\right)\mathbf{p} + \sigma_n^2\mathbf{e}, \tag{3}$$

where $\mathbf{p} = \left[\sigma_{s,1}^2, \ldots, \sigma_{s,K}^2\right]^T$, and $\mathbf{e} = \mathrm{vec}\left\{\mathbf{I}_N\right\}$. Based on the NA geometry, each column of $\mathbf{A}^*(\boldsymbol{\theta}) \odot \mathbf{A}(\boldsymbol{\theta})$ should have only $N_{\mathrm{t}} = 2d_N + 1$ different entries. Thus, the repeated items (after their first occurrence) will be removed in conventional methods. Then, we sort the remaining items to obtain an augmented array manifold, i.e., $\bar{\mathbf{A}} = \left[\bar{\mathbf{a}}(\theta_1), \ldots, \bar{\mathbf{a}}(\theta_K)\right] \in \mathbb{C}^{N_{\mathrm{t}} \times K}$, hereafter the dependence on $\boldsymbol{\theta}$ is removed for notational convenience. In $\bar{\mathbf{A}}$, for $k \in \{1, 2, \ldots, K\}$,

$$\bar{\mathbf{a}}(\theta_k) = \Big[e^{-j\pi d_N \sin\theta_k}, e^{-j\pi(d_N-1)\sin\theta_k}, \ldots, 1, \ldots, e^{j\pi(d_N-1)\sin\theta_k}, e^{j\pi d_N \sin\theta_k}\Big]^T \tag{4}$$

is the steering vector of an extended virtual ULA with sensor positions $\mathcal{P}_{N_{\mathrm{t}}} = \{-d_N, -(d_N-1), \ldots, -1, 0, 1, \ldots, d_N\}$.

Accordingly, the data vector extracted from $\mathbf{r}$ reads[1]

$$\bar{\mathbf{r}} = \bar{\mathbf{A}}\mathbf{p} + \sigma_n^2\mathbf{i} \in \mathbb{C}^{N_{\mathrm{t}} \times 1}, \tag{5}$$

where $\mathbf{i}$ is the $\bar{N}$th ($\bar{N} = d_N + 1$) column of $\mathbf{I}_{N_{\mathrm{t}}}$. Now, $\bar{\mathbf{r}}$ behaves like a measurement sample of the ULA with positions $\mathcal{P}_{N_{\mathrm{t}}}$. In order to estimate the K DOA parameters, we will construct a rank-K matrix and then exploit its eigenstructure to enable subspace methods.

[1] Since the sample covariance matrix $\hat{\mathbf{R}}$ is estimated based on a limited number of snapshots in practice, those theoretically repeated items in $\hat{\mathbf{r}}$ generally have different values. Therefore, to make full use of the second-order statistical information of the array data, we can average the items with the same lag to achieve refined estimates.

3. ALGORITHM DEVELOPMENT

The SS technique is a powerful tool for the above purpose. To formulate a unified expression, we consider the general case where $\bar{\mathbf{r}}$ is divided into I overlapping segments ($I = 1, 2, \ldots, \bar{N}$). The ith ($i = 1, 2, \ldots, I$) segment $\bar{\mathbf{r}}_{I,i}$ spans from the ith to $(i + N_{\mathrm{t}} - I)$th entries of $\bar{\mathbf{r}}$, written as

$$\bar{\mathbf{r}}_{I,i} = \tilde{\mathbf{A}}_I\boldsymbol{\Phi}^{i-1}\mathbf{p} + \sigma_n^2\mathbf{i}_{I,i} = \tilde{\mathbf{A}}_I\mathbf{R}_s\boldsymbol{\phi}_{i-1} + \sigma_n^2\mathbf{i}_{I,i}, \tag{6}$$

where $\tilde{\mathbf{A}}_I$ is composed of the first $N_{\mathrm{t}} - I + 1$ rows of $\bar{\mathbf{A}}$, $\boldsymbol{\Phi} = \mathrm{diag}\left\{e^{j\pi\sin\theta_1}, e^{j\pi\sin\theta_2}, \ldots, e^{j\pi\sin\theta_K}\right\}$, $\mathbf{i}_{I,i}$ consists of the ith to $(i + N_{\mathrm{t}} - I)$th elements in $\mathbf{i}$, and $\boldsymbol{\phi}_{i-1} = \mathrm{diag}\left\{\boldsymbol{\Phi}^{i-1}\right\}$.

Then, we rearrange $\{\bar{\mathbf{r}}_{I,i}\}_{i=1}^{I}$ in the following fashion to get the matrix $\bar{\mathbf{R}}_I$ of size $(N_{\mathrm{t}} - I + 1) \times I$:

$$\bar{\mathbf{R}}_I = \begin{bmatrix}\bar{\mathbf{r}}_{I,I} & \bar{\mathbf{r}}_{I,I-1} & \cdots & \bar{\mathbf{r}}_{I,1}\end{bmatrix} = \mathbf{Q}_I + \mathbf{M}_I, \tag{7}$$

where $\mathbf{Q}_I$ and $\mathbf{M}_I$ are, respectively, the signal- and noise-related terms with the smoothing parameter I, i.e.,

$$\mathbf{Q}_I = \tilde{\mathbf{A}}_I\mathbf{R}_s\mathbf{B}_I^H, \tag{8}$$

$$\mathbf{M}_I = \sigma_n^2\begin{bmatrix}\mathbf{i}_{I,I} & \mathbf{i}_{I,I-1} & \cdots & \mathbf{i}_{I,1}\end{bmatrix}, \tag{9}$$

in which $\mathbf{B}_I^H = \left[\boldsymbol{\phi}_{I-1}, \boldsymbol{\phi}_{I-2}, \ldots, \boldsymbol{\phi}_0\right]$, and we can find that

$$\mathbf{B}_I = \begin{bmatrix} e^{-j\pi(I-1)\sin\theta_1} & \cdots & e^{-j\pi(I-1)\sin\theta_K} \\ \vdots & \ddots & \vdots \\ e^{-j\pi\sin\theta_1} & \cdots & e^{-j\pi\sin\theta_K} \\ 1 & \cdots & 1 \end{bmatrix}. \tag{10}$$

With these formulas, our goal is to find the possible optimized structures of $\bar{\mathbf{R}}_I$ for NA processing.

3.1. Review on SS-MUSIC

First, taking into account the common case of $I = \bar{N}$, we can readily demonstrate that $\tilde{\mathbf{A}}_{\bar{N}}$ and $\mathbf{B}_{\bar{N}}$ will share the same expression. Meanwhile, $\mathbf{M}_I$ will become $\sigma_n^2\mathbf{I}_{\bar{N}}$. At this time,

$$\bar{\mathbf{R}}_{\bar{N}} = \tilde{\mathbf{A}}_{\bar{N}}\mathbf{R}_s\tilde{\mathbf{A}}_{\bar{N}}^H + \sigma_n^2\mathbf{I}_{\bar{N}}, \tag{11}$$

which can be regarded as an $\bar{N} \times \bar{N}$ covariance matrix corresponding to the ULA with $\bar{N}$ sensors located at $\mathcal{P}_{\bar{N}} = \{-d_N, -(d_N - 1), \ldots, 0\}$. Performing EVD on $\bar{\mathbf{R}}_{\bar{N}}$, we can get the noise subspace matrix and then use MUSIC to estimate the K arrival angles. This constitutes the well-known SS-MUSIC algorithm. Obviously, up to $\bar{N} - 1 = d_N$ signals can be resolved, where $d_N = \mathcal{O}\left[N^2\right]$ thanks to the NA geometry. However, the construction in (11) does not take full advantage of the prior knowledge K. Especially when K is much less than d_N, SS-MUSIC can be further improved.

3.2. DOA Estimation Using COPM

To make efficient use of the available aperture, we divide $\bar{\mathbf{r}}$ into $I = K$ segments rather than $I = \bar{N}$, arriving at

$$\bar{\mathbf{R}}_K = \tilde{\mathbf{A}}_K \mathbf{R}_s \mathbf{B}_K^H + \mathbf{M}_K \in \mathbb{C}^{\widetilde{N}\times K}, \tag{12}$$

where $\widetilde{N} = N_{\mathrm{t}} - K + 1$. Clearly, due to the Vandermonde structures of $\tilde{\mathbf{A}}_K$ and $\mathbf{B}_K$, $\mathbf{Q}_K$ (the first term in (12)) is a rank-K matrix suitable for subspace methods. Inspired by this observation, we propose an SMWE-type DOA estimation algorithm (i.e., COPM), whose core idea is to find the noise subspace orthogonal to the column space of $\tilde{\mathbf{A}}_K$. A direct comparison between $\tilde{\mathbf{A}}_K$ and $\tilde{\mathbf{A}}_{\bar{N}}$ shows that the former possesses a larger aperture, implying the better performance of COPM than SS-MUSIC. More mathematically, we introduce the propagator matrix $\mathbf{P} \in \mathbb{C}^{(\widetilde{N}-K)\times K}$, which is a linear operator depending on the partition of $\tilde{\mathbf{A}}_K$ and is defined as

$$\mathbf{P}\tilde{\mathbf{A}}_{K,1} = \tilde{\mathbf{A}}_{K,2}, \tag{13}$$

where $\tilde{\mathbf{A}}_{K,1}$ and $\tilde{\mathbf{A}}_{K,2}$ are, respectively, the first K rows and remaining $\widetilde{N} - K$ rows of $\tilde{\mathbf{A}}_K$. Then, based on the definition of $\mathbf{E} = \left[\mathbf{P}^*, -\mathbf{I}_{\widetilde{N}-K}\right]^T \in \mathbb{C}^{\widetilde{N}\times(\widetilde{N}-K)}$, it can be verified that

$$\mathbf{E}^H \tilde{\mathbf{A}}_K = \mathbf{P}\tilde{\mathbf{A}}_{K,1} - \mathbf{I}_{\widetilde{N}-K}\tilde{\mathbf{A}}_{K,2} = \mathbf{0}. \tag{14}$$

The above equation implies that $\mathbf{E}$ is equivalent to the noise subspace matrix because its columns are orthogonal to the steering vectors in $\tilde{\mathbf{A}}_K$. To estimate the propagator $\mathbf{P}$, we first consider the noise-free case, which means that $\mathbf{M}_K$ has been removed. Please note that such an assumption is also necessary for some related works [3, 5, 19–21]. Focusing on $\bar{\mathbf{R}}_K$, we can partition it into $\bar{\mathbf{R}}_{K,1} \in \mathbb{C}^{K\times K}$ and $\bar{\mathbf{R}}_{K,2} \in \mathbb{C}^{(\widetilde{N}-K)\times K}$, which are related according to (13) as

$$\bar{\mathbf{R}}_K = \begin{bmatrix}\bar{\mathbf{R}}_{K,1}\\ \bar{\mathbf{R}}_{K,2}\end{bmatrix} = \begin{bmatrix}\tilde{\mathbf{A}}_{K,1}\\ \tilde{\mathbf{A}}_{K,2}\end{bmatrix}\mathbf{\Omega} = \begin{bmatrix}\tilde{\mathbf{A}}_{K,1}\\ \mathbf{P}\tilde{\mathbf{A}}_{K,1}\end{bmatrix}\mathbf{\Omega}, \tag{15}$$

where $\mathbf{\Omega} = \mathbf{R}_s\mathbf{B}_K^H \in \mathbb{C}^{K\times K}$. Following (15), we have $\mathbf{P}\bar{\mathbf{R}}_{K,1} = \bar{\mathbf{R}}_{K,2}$. Hence, the propagator $\mathbf{P}$ can be estimated as $\hat{\mathbf{P}} = \bar{\mathbf{R}}_{K,2}\bar{\mathbf{R}}_{K,1}^{-1}$, which will be used to construct the noise subspace matrix $\hat{\mathbf{E}}$. Subsequently, based on the orthogonality in (14), we define the spectrum function of COPM:

$$f(\theta) = \left(\tilde{\mathbf{a}}^H(\theta)\mathbf{\Pi}_{\hat{\mathbf{E}}}\tilde{\mathbf{a}}(\theta)\right)^{-1}, \tag{16}$$

where $\mathbf{\Pi}_{\hat{\mathbf{E}}} = \hat{\mathbf{E}}\left(\hat{\mathbf{E}}^H\hat{\mathbf{E}}\right)^{-1}\hat{\mathbf{E}}^H$ is the orthogonal projector, and $\tilde{\mathbf{a}}(\theta) = \left[e^{-j\pi d_N \sin\theta}, e^{-j\pi(d_N-1)\sin\theta}, \ldots, e^{j\pi(d_N-K+1)\sin\theta}\right]^T$. Then, we can estimate the DOAs by searching the first K maxima of (16). Notably, computing $\mathbf{\Pi}_{\hat{\mathbf{E}}}$ involves the inversion of the $(\widetilde{N}-K)\times(\widetilde{N}-K)$ matrix $\hat{\mathbf{E}}^H\hat{\mathbf{E}}$. To alleviate the computational burden of this nonlinear operation, we keep the Woodbury matrix identity in mind and transform $\mathbf{\Pi}_{\hat{\mathbf{E}}}$ into $\mathbf{\Pi}_{\hat{\mathbf{E}}} = \hat{\mathbf{E}}\big(\mathbf{I}_{\widetilde{N}-K} - \hat{\mathbf{P}}(\mathbf{I}_K + \hat{\mathbf{P}}^H\hat{\mathbf{P}})^{-1}\hat{\mathbf{P}}^H\big)\hat{\mathbf{E}}^H$. In this way, the inversion only takes place on the $K\times K$ matrix $\mathbf{I}_K + \hat{\mathbf{P}}^H\hat{\mathbf{P}}$.

Complexity issues: The proposed method avoids EVD procedures. Instead, the two nonlinear operations contained in COPM are the inversions of $\bar{\mathbf{R}}_{K,1}$ and $\mathbf{I}_K + \hat{\mathbf{P}}^H\hat{\mathbf{P}}$, which are used to estimate the propagator and construct the orthogonal projection matrix, respectively. Note that both matrices are of size $K \times K$, resulting in a complexity of $\mathcal{O}[K^3]$. Compared with the complexity $\mathcal{O}[\bar{N}^3]$ caused by the EVD of $\bar{\mathbf{R}}_{\bar{N}}$ (11) in SS-MUSIC, the computational advantage of our method is considerable, especially for a relatively small K.

3.3. Projection-Based Noise Elimination

Until now, the problem of noise elimination still deserves further discussion. In fact, traditional denoising methods, e.g., the eigenvalue-based (EV) estimation approach [12], generally involve the EVD of the high-dimensional matrix $\bar{\mathbf{R}}_{\bar{N}}$, thus defeating the purpose of computational simplicity. Unlike EV methods, we propose an SMWE-type noise cancellation method, i.e., PNEM, which will be conducive to improving the COPM performance at high noise levels.

First, let us have a closer look at the explicit expression of $\mathbf{M}_I$ in (9). That is, $\mathbf{M}_I = \left[\mathbf{0}_{\bar{N}-I,I}^T, \sigma_n^2\mathbf{I}_I, \mathbf{0}_{\bar{N}-I,I}^T\right]^T$, which embodies that even in the noisy case, only the $(\bar{N}-I+1)$th to $\bar{N}$th rows of $\bar{\mathbf{R}}_I$ will be impacted by $\sigma_n^2\mathbf{I}_I$ in theory. With this observation, we make the following partitions:

$$\bar{\mathbf{R}}_I = \begin{bmatrix}\bar{\mathbf{R}}_I^{(1)}\\ \bar{\mathbf{R}}_I^{(2)}\\ \bar{\mathbf{R}}_I^{(3)}\end{bmatrix}\begin{matrix}\}\bar{N}-I\\ \}I\\ \}\bar{N}-I\end{matrix} = \begin{bmatrix}\mathbf{Q}_I^{(1)}\\ \mathbf{Q}_I^{(2)}\\ \mathbf{Q}_I^{(3)}\end{bmatrix} + \begin{bmatrix}\mathbf{0}_{\bar{N}-I,I}\\ \sigma_n^2\mathbf{I}_I\\ \mathbf{0}_{\bar{N}-I,I}\end{bmatrix}, \tag{17}$$

where $\mathbf{Q}_I^{(l)} = \tilde{\mathbf{A}}_I^{(l)}\mathbf{R}_s\mathbf{B}_I^H$, $l = 1, 2, 3$, and the forms of $\tilde{\mathbf{A}}_I^{(l)}$ can be clearly obtained from (17). Then, we notice that (i) $\mathbf{B}_I$ in (10) can be viewed as an $I \times K$ manifold matrix. If $I > K$, $\mathbf{B}_I$ will have full column rank, which corresponds to an overdetermined case. (ii) If $\bar{N} - I \geq K$, the columns of $\left(\bar{\mathbf{R}}_I^{(1)}\right)^H$, $\left(\bar{\mathbf{R}}_I^{(3)}\right)^H$, and $\mathbf{B}_I$ will span the same subspace.

Building on these insights and keeping the assumptions of $I > K$ and $\bar{N} - I \geq K$ in mind, we set I to $\bar{N} - K$. This is because (i) the row dimension of $\mathbf{B}_I$ can reach its maximum value, and (ii) the constraint on the source number (i.e., $I > K$) will be relaxed to the maximum extent possible. Then, the projector onto the orthogonal complement of $\mathbf{B}_{\bar{N}-K}$ will be

$$\mathbf{\Pi}_{\mathbf{B}_{\bar{N}-K}} = \mathbf{I}_{\bar{N}-K} - (\mathbf{R}_{\bar{N}-K}^{(l)})^H\big((\mathbf{R}_{\bar{N}-K}^{(l)})^H\big)^\dagger,\ l = 1, 3,$$

which contains the inversion of a $K \times K$ matrix. To proceed, the noise power can be estimated by [22]

$$\hat{\sigma}_n^2 = \frac{\mathrm{trace}\big\{\bar{\mathbf{R}}_{\bar{N}-K}^{(2)}\mathbf{\Pi}_{\mathbf{B}_{\bar{N}-K}}\big\}}{\mathrm{trace}\left\{\mathbf{\Pi}_{\mathbf{B}_{\bar{N}-K}}\right\}}. \tag{18}$$

Since the explicit theoretical expression of $\mathbf{M}_I$ is clear (9), we can remove $\mathbf{M}_I$ from $\bar{\mathbf{R}}_I$ to isolate $\mathbf{Q}_I$ for noise cancellation.

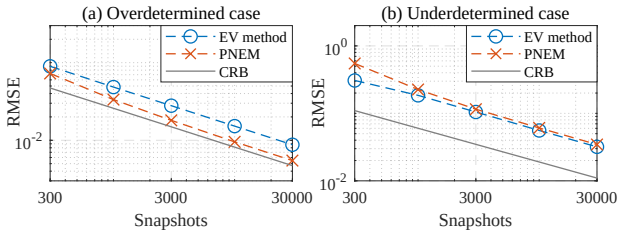

Fig. 1: RMSE of noise power estimate versus snapshot number. (a) overdetermined case. (b) underdetermined case.

Identifiability condition: To satisfy that $I > K$, where $I = \bar{N} - K$, PNEM is applicable to the case of $K < \bar{N}/2$. Owing to the NA geometry, the relationship $\bar{N} = \mathcal{O}\left[N^2\right]$ holds, i.e., our method can still deal with underdetermined cases. But in comparison with the EV method based on $\bar{\mathbf{R}}_{\bar{N}}$, which can accommodate the case of $K < \bar{N}$, our method compromises on identifiability conditions. Nevertheless, it should be mentioned that such a compromise is also inevitable for other SMWE-type denoising approaches, which, moreover, fail to handle underdetermined cases.

4. SIMULATIONS

We consider an 8-element NA with the configuration $\mathcal{P}_8 = \{0, 1, 2, 3, 7, 11, 15, 19\}$. Without loss of generality, we assume that all signals have equal power σ_s^2. The signal-to-noise ratio (SNR) is defined as $\text{SNR} = 10\log_{10}(\sigma_s^2/\sigma_n^2)$.

First, we evaluate the noise power estimation performance of the EV method [12] and the proposed PNEM. Due to $\bar{N}/2 = 10$, PNEM can deal with the case where up to 9 sources are present. First, considering an overdetermined case, we assume that two signals with -5 dB SNR come from $\boldsymbol{\theta} = \{-30°, 20°\}$. Treating the root-mean-square error (RMSE) of $\hat{\sigma}_n^2$ as a function of the snapshot number M, we obtain Fig. 1(a) based on 10000 independent Monte-Carlo trials. Meanwhile, the Cramér-Rao bound [23] is given as the performance benchmark. We can find that PNEM provides more accurate estimates than the EV method, which is attributed to the construction of $\bar{\mathbf{R}}_{\bar{N}-K}$. Then, we move on to the underdetermined case, where the DOAs of $K = 9$ signals are uniformly distributed from $-50°$ to $70°$ with an interval of $15°$. The other settings remain unchanged. We plot the RMSE curves in Fig. 1(b), which shows that the estimation accuracy of PNEM gets closer to that of the EV method as the snapshot number increases, meanwhile benefiting from a slighter computational burden. Fig. 1 illustrates that PNEM is suitable for the case where K is relatively small.

Next, we check the estimation performance of COPM by comparing it with the widely used SS-MUSIC and the pseudo-noise subspace-based OPM (PNS-OPM) [21]. The RMSE of $\boldsymbol{\theta}$ is calculated by $\sqrt{\frac{1}{KL}\sum_{k=1}^{K}\sum_{l=1}^{L}\left(\hat{\theta}_{k,l} - \theta_k\right)^2}$, where $L = 1 \times 10^4$ is the number of Monte-Carlo trials, and $\hat{\theta}_{k,l}$ is the estimate of θ_k in the lth trial. For a fair comparison,

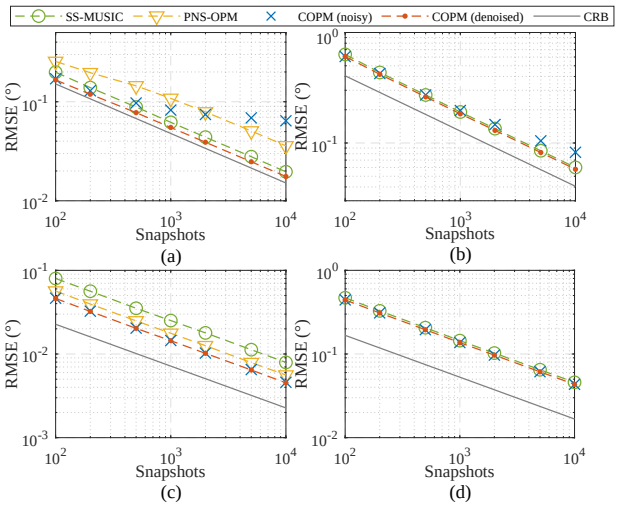

Fig. 2: RMSE performance comparison. (a) overdetermined case, -5 dB. (b) underdetermined case, -5 dB. (c) overdetermined case, 10 dB. (d) underdetermined case, 10 dB.

PNS-OPM will be implemented after using PNEM to eliminate noise. Moreover, it directly extracts the noise subspace from the covariance matrix corresponding to the physical array, thus failing to work in underdetermined conditions. This means that the major advantage of NAs, i.e., the enhanced degrees of freedom, is sacrificed in PNS-OPM. In the experiments, for both the overdetermined ($\boldsymbol{\theta} = \{0°, 13°\}$) and underdetermined ($\boldsymbol{\theta}$ is consistent with that in Fig. 1(b)) cases, the low SNR (-5 dB) and high SNR (10 dB) scenarios are separately considered in Figs. 2(a)-(d). For a comprehensive analysis, the performance of COPM is evaluated in both noisy and denoised cases, and noise cancellation is achieved by PNEM. As can be seen, after eliminating noise, COPM exhibits obvious advantages in estimation accuracy for all simulation environments. This can be explained by the fact that $\tilde{\mathbf{A}}_K$ has a larger aperture than $\tilde{\mathbf{A}}_{\bar{N}}$. Notably, even without denoising processing, the performance degradation of COPM is very weak at high SNRs, as shown in Figs. 2(c) and (d). But when it comes to the low SNR regime, COPM without denoising suffers from a loss of accuracy, especially with a large number of snapshots.

5. CONCLUSION

For NAs, two co-array-based SMWE-type methods, i.e., COPM and PNEM, are proposed as computationally efficient schemes for DOA estimation and noise elimination, respectively. In comparison with the EV method, PNEM provides more accurate estimates in overdetermined cases and shows comparable performance in underdetermined cases. Compared with SS-MUSIC and PNS-OPM, owing to the efficient use of the co-array aperture, COPM exhibits advantages in estimation precision after eliminating noise. Additionally, even without denoising processing, the simulations demonstrate that COPM has almost no loss of accuracy at high SNRs.

References

[1] Piya Pal and Palghat P Vaidyanathan, "Nested arrays: A novel approach to array processing with enhanced degrees of freedom," *IEEE Trans. Signal Process.*, vol. 58, no. 8, pp. 4167–4181, Aug. 2010.

[2] Keyong Han and Arye Nehorai, "Nested vector-sensor array processing via tensor modeling," *IEEE Trans. Signal Process.*, vol. 62, no. 10, pp. 2542–2553, May 2014.

[3] Jin He, Zenghui Zhang, Ting Shu, and Wenxian Yu, "Direction finding of multiple partially polarized signals with a nested cross-diople array," *IEEE Antennas Wirel. Propag. Lett.*, vol. 16, pp. 1679–1682, Feb. 2017.

[4] Jin He, Linna Li, and Ting Shu, "2-D direction finding using parallel nested arrays with full co-array aperture extension," *Signal Process.*, vol. 178, pp. 107795, Jan. 2021.

[5] Xinghao Qu, Yi Lou, Yunjiang Zhao, Yinheng Lu, and Gang Qiao, "Augmented tensor MUSIC for DOA estimation using nested acoustic vector-sensor array," *IEEE Signal Process. Lett.*, vol. 29, pp. 1624–1628, Jul. 2022.

[6] Yi Lou, Xinghao Qu, Dawei Wang, and Julian Cheng, "Direction-of-arrival estimation for nested acoustic vector-sensor arrays using quaternions," *IEEE Trans. Geosci. Remote Sens.*, vol. 61, pp. 1–14, May 2023.

[7] Chun-Lin Liu and P. P. Vaidyanathan, "Remarks on the spatial smoothing step in coarray MUSIC," *IEEE Signal Process. Lett.*, vol. 22, no. 9, pp. 1438–1442, Sep. 2015.

[8] Zhi Zheng and Shilin Mu, "Two-dimensional DOA estimation using two parallel nested arrays," *IEEE Commun. Lett.*, vol. 24, no. 3, pp. 568–571, Mar. 2020.

[9] Jin He, Zenghui Zhang, Ting Shu, and Wenxian Yu, "Sparse nested array with aperture extension for high accuracy angle estimation," *Signal Process.*, vol. 176, pp. 107700, Nov. 2020.

[10] Jianfeng Li, Yi He, Penghui Ma, Xiaofei Zhang, and Qihui Wu, "Direction of arrival estimation using sparse nested arrays with coprime displacement," *IEEE Sensors J.*, vol. 21, no. 4, pp. 5282–5291, Feb. 2021.

[11] Zhi Zheng and Shilin Mu, "2-D direction finding with pair-matching operation for L-shaped nested array," *IEEE Commun. Lett.*, vol. 25, no. 3, pp. 975–979, Mar. 2021.

[12] Jin He, Linna Li, and Ting Shu, "Sparse nested arrays with spatially spread square acoustic vector sensors for high-accuracy underdetermined direction finding," *IEEE Trans. Aerosp. Electron. Syst.*, vol. 57, no. 4, pp. 2324–2336, Feb. 2021.

[13] Lei Wang, Chunhui Ren, Renting Liu, and Zhi Zheng, "Direction-of-arrival estimation for nested array using mixed-resolution ADCs," *IEEE Commun. Lett.*, vol. 26, no. 8, pp. 1868–1872, Aug. 2022.

[14] Sylvie Marcos, Alain Marsal, and Messaoud Benidir, "The propagator method for source bearing estimation," *Signal Process.*, vol. 42, no. 2, pp. 121–138, 1995.

[15] Guangmin Wang, Jingmin Xin, Nanning Zheng, and Akira Sano, "Computationally efficient subspace-based method for two-dimensional direction estimation with L-shaped array," *IEEE Trans. Signal Process.*, vol. 59, no. 7, pp. 3197–3212, Jul. 2011.

[16] Weiliang Zuo, Jingmin Xin, Nanning Zheng, and Akira Sano, "Subspace-based localization of far-field and near-field signals without eigendecomposition," *IEEE Trans. Signal Process.*, vol. 66, no. 17, pp. 4461–4476, Sep. 2018.

[17] Yi Lou, Gang Qiao, Xinghao Qu, and Feng Zhou, "Computationally efficient two-dimensional DOA estimation algorithm based on quaternion theory," *IEEE Signal Process. Lett.*, vol. 28, pp. 1764–1768, Aug. 2021.

[18] Yi Lou, Xinghao Qu, Yinheng Lu, and Gang Qiao, "Quaternion-based two-dimensional DOA estimation for coherent underwater sources without eigendecomposition," *IEEE Access*, vol. 9, pp. 104142–104153, Jul. 2021.

[19] Xiaodong Han, Ting Shu, Jin He, and Wenxian Yu, "Polarization-angle-frequency estimation with linear nested vector sensors," *IEEE Access*, vol. 6, pp. 36916–36926, 2018.

[20] Ting Shu, Jin He, Xiaodong Han, Xiaoming Li, and Kai-Bor Yu, "Joint DOA and degree-of-polarization estimation of partially-polarized signals using nested arrays," *IEEE Commun. Lett.*, vol. 24, no. 10, pp. 2182–2186, Oct. 2020.

[21] Xiangdong Huang, Xiaoqing Yang, Lu Cao, and Wei Lu, "Pseudo noise subspace based DOA estimation for unfolded coprime linear arrays," *IEEE Wireless Commun. Lett.*, vol. 10, no. 11, pp. 2335–2339, Nov. 2021.

[22] J. Sanchez-Aranjo and S. Marcos, "Statistical analysis of the propagator method for DOA estimation without eigendecomposition," in *Proc. IEEE 8th Workshop Statistical Signal Array Process.*, Jun. 1996, pp. 570–573.

[23] Mianzhi Wang and Arye Nehorai, "Coarrays, MUSIC, and the Cramér-Rao bound," *IEEE Trans. Signal Process.*, vol. 65, no. 4, pp. 933–946, Feb. 2017.